2012

Flux distribution in Fe-based superconducting materials by magneto-optical imaging

Zhi Wei Lin
University of Technology, Sydney

Jian Guo Zhu
University of Technology, Sydney

You Guang Guo
University Of Technology Sydney

Xiaolin Wang
University of Wollongong, xiaolin@uow.edu.au

S X. Dou
University of Wollongong, shi@uow.edu.au

See next page for additional authors

Flux distribution in Fe-based superconducting materials by magneto-optical imaging

Abstract

"This paper presents the magnetic flux distributions in Fe-based superconducting materials including single crystal of $Ba(Fe_{1.9}Ni_{0.1})As_2$ and $Ba(Fe_{1.8}Co_{0.2})As_2$, as well as polycrystalline $SmFeO_{0.75}F_{0.2}As$ by means of magneto-optical imaging (MOI) technique. The single crystals were grown out of FeAs flux while polycrystalline sample was grown by hot-press. A MOI film with in-plan magnetization was used to visualize flux distributions at the sample surface. A series of magneto-optical images was taken when the samples were zero-field cooled and field cooled. The flux behavior, including penetration into and expelling from the samples, as well as pinning properties were studied. When external fields increase, flux is completely shielded from the crystals, then, gradually penetrates toward the crystal center from the edge. For polycrystalline sample, Meissner state was observed at very low field. With increasing the field further, flux penetrates into the sample easily along grain boundary, then into grain. Compared with high-T_C cuprates, it is found that the flux distributions in Fe-based superconducting materials are very similar to that in high-T_C cuprates with strong pinning strength.

Keywords

fe, magneto, distribution, flux, optical, materials, superconducting, imaging

Disciplines

Engineering | Physical Sciences and Mathematics

Publication Details

Lin, Z. Wei., Zhu, J. Guo., Guo, Y. Guang., Wang, X. Lin., Dou, S. Xue., Johansen, T. H., Shi, X. & Choi, K. Y. (2012). Flux distribution in Fe-based superconducting materials by magneto-optical imaging. Journal of Applied Physics, 111 (7), 07E143-1-07E143-3.

Authors

Zhi Wei Lin, Jian Guo Zhu, You Guang Guo, Xiaolin Wang, S X. Dou, Tom H. Johansen, Xun Shi, and K Y. Choi

Flux distribution in Fe-based superconducting materials by magneto-optical imaging

Zhi Wei Lin, Jian Guo Zhu, You Guang Guo, Xiao Lin Wang, Shi Xue Dou et al.

Citation: J. Appl. Phys. **111**, 07E143 (2012); doi: 10.1063/1.3679353
View online: http://dx.doi.org/10.1063/1.3679353
View Table of Contents: http://jap.aip.org/resource/1/JAPIAU/v111/i7
Published by the American Institute of Physics.

Flux distribution in Fe-based superconducting materials by magneto-optical imaging

Zhi Wei Lin,[1,a)] Jian Guo Zhu,[1] You Guang Guo,[1] Xiao Lin Wang,[2] Shi Xue Dou,[2] Tom H. Johansen,[2,3,4] Xun Shi,[5] and K. Y. Choi[6]
[1]*University of Technology, PO Box 123, Broadway, Sydney, New South Wales 2007, Australia.*
[2]*Institute for Superconducting and Electronic Materials, Innovation Campus, University of Wollongong, North Wollongong, New South Wales 2500, Australia*
[3]*Department of Physics, University of Oslo, P.O. Box 1048, Blindern, N-0316 Oslo, Norway*
[4]*Centre for Advanced Study, Norwegian Academy of Science and Letters, N-0271, Oslo, Norway*
[5]*CAS Key Laboratory of Materials for Energy Conversion, Shanghai Institute of Ceramics, Chinese Academy of Sciences, 1295 Dingxi Road, Shanghai 200050, China*
[6]*Frontier Physics Research Division and Department of Physics and Astronomy, Seoul National University, Seoul 151-747, South Korea*

(Presented 3 November 2011; received 28 September 2011; accepted 21 November 2011; published online 12 March 2012)

This paper presents the magnetic flux distributions in Fe-based superconducting materials including single crystal of $Ba(Fe_{1.9}Ni_{0.1})As_2$ and $Ba(Fe_{1.8}Co_{0.2})As_2$, as well as polycrystalline $SmFeO_{0.75}F_{0.2}As$ by means of magneto-optical imaging (MOI) technique. The single crystals were grown out of FeAs flux while polycrystalline sample was grown by hot-press. A MOI film with in-plan magnetization was used to visualize flux distributions at the sample surface. A series of magneto-optical images was taken when the samples were zero-field cooled and field cooled. The flux behavior, including penetration into and expelling from the samples, as well as pinning properties were studied. When external fields increase, flux is completely shielded from the crystals, then, gradually penetrates toward the crystal center from the edge. For polycrystalline sample, Meissner state was observed at very low field. With increasing the field further, flux penetrates into the sample easily along grain boundary, then into grain. Compared with high-T_c cuprates, it is found that the flux distributions in Fe-based superconducting materials are very similar to that in high-T_c cuprates with strong pinning strength. © *2012 American Institute of Physics*. [doi:10.1063/1.3679353]

I. INTRODUCTION

New-discovered superconducting materials in oxypnictide phase, $LaFeAs(O_{1-x}F_x)$[1,2] show promising applications due to their extremely high upper critical field.[3,4] Superconductivity has been found in a wide variety of compounds, for example, the oxypnictide of $LaFeAsO_{1-x}F_x$, their oxygen-free parent compounds of $BaFe_2As_2$,[5] LiFeAs,[6] and $FeTe_xSe_{1-x}$.[7–9] Visualization of flux properties in different compounds will provide fundamental understanding of the superconducting mechanisms and pave the way for applications.

Superconducting Quantum Interference Devices (SQUID) and Vibrating Sample Magnetometers (VSM) normally study collective information of magnetic properties in whole volume of the sample. Magneto-optical imaging (MOI) technique can visualize local and real-time magnetic flux distribution in the sample with spatial resolution of 3 μm using in-plane magnetization indicator film.[10–12] This paper presents flux distributions at different Fe-based superconducting samples using MOI technique when samples were zero field cooled (ZFC) or field cooled (FC). Three samples were studied, for example, single crystalline $Ba(Fe_{1.8}Co_{0.2})As_2$ and $Ba(Fe_{1.9}Ni_{0.1})As_2$, as well as polycrystalline $SmFe(O_{0.75}F_{0.2})As$.

[a)]Author to whom correspondence should be addressed. Electronic mail: jacklin@eng.uts.edu.au.

II. EXPERIMENTAL DETAIL

The $Ba(Fe_{1.8}Co_{0.2})As_2$ and $Ba(Fe_{1.9}Ni_{0.1})As_2$ single crystals were grown out of Fe-As flux using standard high-temperature solution growth technique.[13] The polycrystalline $SmFeO_{0.75}F_{0.2}As$ was grown by hot press at 1300 °C and 4.0 GPa.[14]

A series of magneto-optical images was taken at different magnetic fields or temperatures using home-made MOI system,[15] so that the flux penetration can be visualized. An indicator film[16] with in-plan magnetization was carefully placed on polished sample surface with minor pressure to improve image quality.

III. RESULTS AND DISCUSSION

A. $Ba(Fe_{1.8}Co_{0.2})As_2$ single crystal

Resistivity and magnetization measurements show $T_c = 25$ K. The crystal was ZFC to 4.2 K, then, external magnetic field was applied. Figure 1 shows magneto-optical images in the indicator film at different fields. Figure 2 shows the flux profiles along the red line indicated in Fig. 1(b). The scratch in the indicator film causes unexpected drop at left side profile. It can be seen that magnetic flux was completely shielded from the crystal at 40 Oe, that is, the crystal was in Meissner state. With increasing the fields flux started penetration into the crystal from the edges, but the

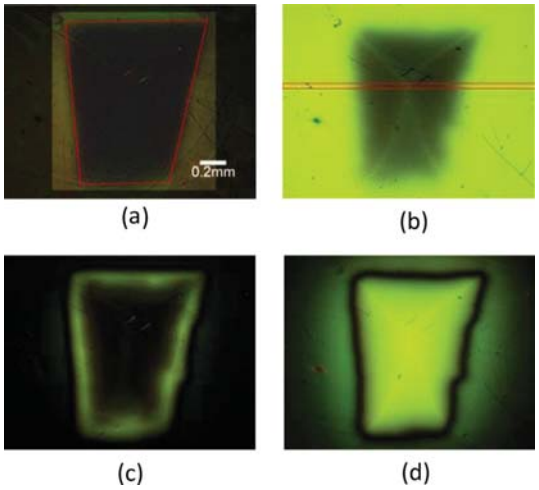

FIG. 1. (Color online) Magneto-optical images when fields increased to (a) 40 Oe, (b) 800 Oe, (c) then decreased to zero. The crystal was cooled to 4.2 K in the application of 800 Oe, (d) then field reduced to zero. The red square illustrates sample edge and Fig. 1(a) is contrast-enhanced.

flux-free region still existed in the center of the crystal. The flux front moved gradually toward the center of the sample when field was increasing. Such front motion is clearly shown in the profiles. However, full penetration was not observed since the field generated by the electromagnet was limited to 800 Oe, obviously less than full penetration field. The critical current, J_c, can be estimated from the position of the flux front[17] at $H_a = 800$ Oe, $J_c = H_a\pi/\{[\cosh^{-1}(a/b)]$ where a = 0.7 mm is half width of the crystal, b = 0.4 mm the position of flux front, d = 0.1 mm the thickness of the crystal. $J_c = 1.7 \times 10^9$ A/m^2 is obtained. As field decreased, the flux only close to the edges escaped from the crystal while the flux far to the edge was pinned in the crystal. The observed flux behavior in the crystal are similar to that in high-T_c cuprates[18] and are consistent with Bean model[19] and theoretical calculations.[17,18] However, the theoretical peaks at the edges were not clearly observed in this work since the edges of the crystal were not well defined and a spatial gap existed inevitably between the indicator film and the crystal surface.[20]

Figure 1(d) shows image taken when the crystal was FC to 4.2 K in the application of external field of 800 Oe, then the

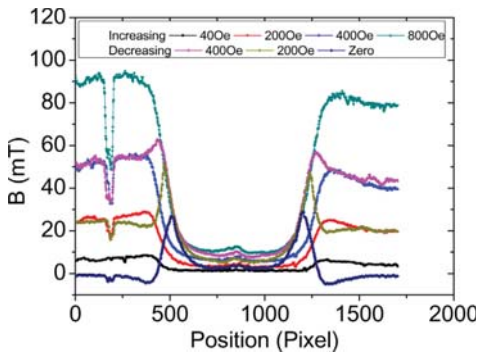

FIG. 2. (Color online) Flux profile along the red line shown in Fig. 1(b) when applied field increased to 40 Oe, 200 Oe, 400 Oe and 800 Oe, following by decreasing to 400 Oe, 200 Oe and zero.

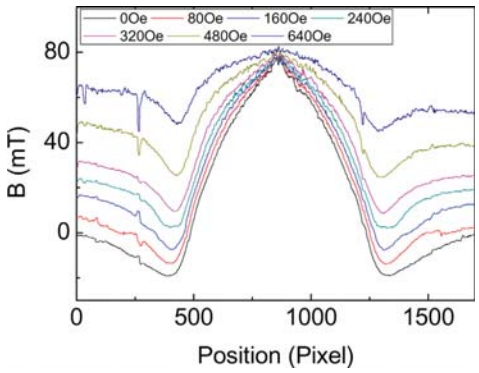

FIG. 3. (Color online) Flux profile for the sample FC to 4.2 K in 800 Oe followed by reducing field to zero.

field reduced to zero. It clearly shows that the flux is pinned in the crystal when external field reduces to zero. Figure 3 shows flux profiles at the different decreasing fields. With decreasing field, the introduced flux continuously left the crystal, forming a density gradient in the crystal. The flux even changed polarity when the field approached to zero. This phenomenon is quite similar with the high-T_c copper oxides.[18] Following by increasing temperature, the pinning was becoming weak. At 25 K the crystal lost superconductivity.

B. $Ba(Fe_{1.9}Ni_{0.1})As_2$ single crystal

Resistivity measurement shows that T_c of the crystal is 18.8 K. Figure 4 presents magneto-optical images taken by another MOI system when the crystal was zero-field cooled to 10 K, followed by increasing external fields parallel to the

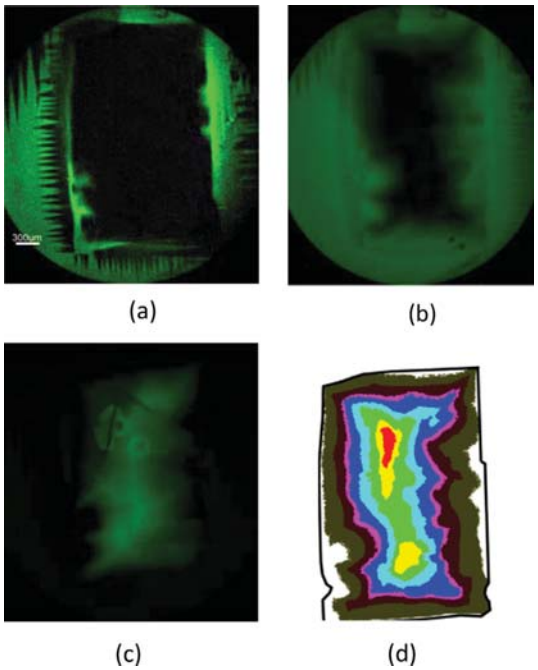

FIG. 4. (Color online) Magneto-optical images taken at 10 K with field increasing to (a) 83 Oe, (b) 354 Oe, and (c) remanent state after field up to 1700 Oe. (d) Color coded flux-free region for applied field of 109 Oe, 135 Oe, 265 Oe, 299 Oe, 354 Oe, 430 Oe, 502 Oe, and 531 Oe. The black line is outline of the crystal.

c-direction. The contrast of Fig. 4(a) only was enhanced using imaging edit software. The tooth pattern domain resulted from the field parallel to the indicator film. Some defects in the indicator film can be clearly seen. Below 50 Oe the flux was completely shielded from the crystal, and crystal was in the Meissner state. Flux started penetration into the crystal from points along the edge over 60 Oe, as shown in Fig. 4(a) taken at 83 Oe. With increasing magnetic field, flux penetrated into the crystal further. In addition, penetration also occurred along the crystal edges, as shown in Figs. 4(b). At 531 Oe, the salient flux front reached the central region of the crystal, but still there was a small flux-free region. At about 584 Oe, flux entered the whole crystal and flux-free region disappeared. Figure 4(c) is the remanent state after the field increased to 1700 Oe. It clearly shows that the penetrated flux is pinned in the central region of the crystal and flux around the crystal edges escapes from the crystal.

In order to clearly present progress of the flux front moving toward the crystal center, Fig. 4(d) shows color-coded flux-free regions at different fields. Flux penetration first occurs at the defect points along the edges. With increasing field, flux penetration also occurs along the edge, forming irregular shape of flux fronts. As a result, flux penetrated further and flux-free region continuously shrinks. It can also be seen that flux penetrates into the crystal from the defect points, that is lower pinning points, along the edges, but these points are not the starting points of the channels along which the flux can easily enter the crystal, like twin structure in $YBa_2Cu_3O_{7-\delta}$ crystal.[21] These lower pinning points might be caused by crystal structure defects which are randomly distributed in the crystal. As a result of lower pinning points, the shapes of the flux front are irregular.

C. Polycrystalline $SmFe(O_{0.75}F_{0.2})As$

T_c of the polycrystalline sample is 45.7 K. Microscope inspection does not reveal any cracks in the sample. Figure 5 shows the magneto-optical images at ZFC condition. Meissner state was clearly observed at 4.2 K, indicating that the global shielding current flows over the whole sample. As external field increased, flux started to penetrate into the sample initially along intergranular path, but flux was still expelled from individual grains, which are shown as black areas in Fig. 5(a). It is the evidence that the pinning strength in the grain is much stronger than that at the intergranular path. This observation is consistent with magnetization loops where the magnetization peak drops at relatively low field of 8 Oe. The easy flux penetration along the intergranular path was also demonstrated in Fig. 5(b) which was taken after external magnetic field increased to 800 Oe and decreased to zero. It can be noted that the bright areas in Fig. 5(b) are corresponding to the black areas in Fig. 5(a). This indicates that the flux is pinned in the grains while the flux at the intergranular path leaves the sample along the path and the local shielding current around grain is denser than global shielding current due to the inter-grain weak-link.[21,22] Such feature was also observed in cuprate polycrystalline sample.[23]

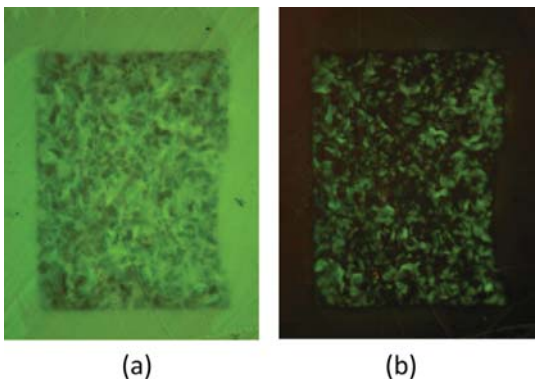

FIG. 5. (Color online) (a) Imaging taken at 160 Oe showing flux penetration easily along intergranular path. (b) Remanent state after field increased to 800 Oe and decreased to zero.

IV. CONCLUSION

The flux behavior, including penetration, escape and pinning feature, in Fe-based superconducting single crystalline $Ba(Fe_{1.8}Co_{0.2})As_2$ and $Ba(Fe_{1.9}Ni_{0.1})As_2$ and polycrystalline $SmFe(O_{0.75}F_{0.2})As$ were visualized by means of magneto-optical imaging technique at zero-field cool and field cool conditions. In general, the flux behaviors in Fe-based superconducting single crystalline are very similar to that in high-T_c cuprates single crystalline and their behaviors can be understood using Bean model. However, the Bean penetration behavior was not observed in polycrystalline sample due to intergranular weak-line between the grains. Flux behavior in Fe-based polycrystalline sample is also similar to that in polycrystalline cuprates.

[1]Y. Kamihara, T. Watanabe, M. Hirano *et al.*, J. Am. Chem. Soc. **130**, 3296 (2008).
[2]H. Takahashi, K. Igawa, K. Arii *et al.*, Nature **453**, 376 (2008).
[3]A. Yamamoto, J. Jiang, C. Tarantini *et al.*, Appl. Phys. Lett. **92**, 252501 (2008).
[4]S. Haindl, M. Kidszun, A. Kauffmann *et al.*, Phys. Rev. Lett. **104**, 077001 (2010).
[5]M. Rotter, M. Tegel, and D. Johrendt, Phys. Rev. Lett. **101**, 107006 (2008).
[6]X. C. Wang, Q. Q. Liu, Y. X. Lv *et al.*, Solid State Commun. **148**, 538 (2008).
[7]F. C. Hsu, J. Y. Luo, K. W. Yeh *et al.*, Proc. Natl. Acad. Sci. U. S. A. **105**, 14262 (2008).
[8]W. D. Si, Z. W. Lin, Q. Jie *et al.*, Appl. Phys. Lett. **95**, 3 (2009).
[9]J. Wen, G. Xu, Z. Xu *et al.*, Phys. Rev. B **80**, 104506 (2009).
[10]R. Prozorov, M. A. Tanatar, E. C. Blomberg *et al.*, Physica C **469**, 667 (2009).
[11]R. Prozorov, M. A. Tanatar, B. Roy *et al.*, Phys. Rev. B **81**, 094509 (2010).
[12]C. J. van der Beek, G. Rizza, M. Konczykowski *et al.*, Physica C **470**, S385 (2010).
[13]A. S. Sefat, R. Jin, M. A. McGuire *et al.*, Phys. Rev. Lett. **101**, 117004 (2008).
[14]Z. W. Lin, Y. J. Li, J. G. Zhu *et al.*, J. Appl. Phys. **107**, 09E114 (2010).
[15]Z. W. Lin, J. G. Zhu, J. J. Zhong *et al.*, J. Appl. Phys. **101**, 09K107 (2007).
[16]L. E. Helseth, R. W. Hansen, E. I. Il'yashenko *et al.*, Phys. Rev. B **64**, 174406 (2001).
[17]E. H. Brandt, and M. Indenbom, Phys. Rev. B **48**, 12893 (1993).
[18]T. Schuster, H. Kuhn, E. H. Brandt *et al.*, Phys. Rev. B **50**, 16684 (1994).
[19]C. P. Bean, Rev. Mod. Phys. **36**, 31 (1964).
[20]Z. W. Lin, J. W. Cochrane, N. E. Lumpkin *et al.*, Physica C **312**, 247 (1999).
[21]Z. W. Lin, G. D. Gu, A. S. Mahmoud *et al.*, Physica C **349**, 95 (2001).
[22]A. Yamamoto, A. A. Polyanskii, J. Jiang *et al.*, Supercond. Sci. Technol. **21**, 095008 (2008).
[23]A. E. Pashitski, A. Gurevich, A. A. Polyanskii *et al.*, Science **275**, 367 (1997).